BIOHYBRID MICROBES

Light-driven fine chemical production in yeast biohybrids

Junling Guo[1*†], Miguel Suástegui[1†], Kelsey K. Sakimoto[2,3], Vanessa M. Moody[4], Gao Xiao[1,5], Daniel G. Nocera[2], Neel S. Joshi[1,5*]

Inorganic-biological hybrid systems have potential to be sustainable, efficient, and versatile chemical synthesis platforms by integrating the light-harvesting properties of semiconductors with the synthetic potential of biological cells. We have developed a modular bioinorganic hybrid platform that consists of highly efficient light-harvesting indium phosphide nanoparticles and genetically engineered *Saccharomyces cerevisiae*, a workhorse microorganism in biomanufacturing. The yeast harvests photogenerated electrons from the illuminated nanoparticles and uses them for the cytosolic regeneration of redox cofactors. This process enables the decoupling of biosynthesis and cofactor regeneration, facilitating a carbon- and energy-efficient production of the metabolite shikimic acid, a common precursor for several drugs and fine chemicals. Our work provides a platform for the rational design of biohybrids for efficient biomanufacturing processes with higher complexity and functionality.

Inorganic-biological hybrid systems combine the light-harvesting efficiency of inorganic systems with established biosynthetic pathways in live cells, thus promising a sustainable and efficient biochemical synthesis platform (*1*, *2*). Comprehensive solar-to-chemical production has been investigated with bioinorganic hybrid systems, including semiconductor-conjugated hydrogenases for biohydrogen production (*3*–*5*), long-wavelength–absorbing nanomaterials integrated into plants for enhanced photosynthetic efficiency (*6*), and photoelectrodes coupled with whole cells for hydrogenation reactions (*7*) as well as atmospheric CO_2 and N_2 fixation (*8*–*11*).

Microorganisms are used in biomanufacturing because of their rapid proliferation and ability to convert renewable carbon sources into higher-value chemicals through genetically programmable multistep catalysis (*12*). In the context of inorganic-biological hybrids, autotrophic bacteria have been investigated intensively, with a focus on simple organic molecules (*7*–*14*). Interfacing heterotrophic organisms with light-harvesting inorganics may provide advantages, such as increased efficiency in the production of high-value chemicals (*15*–*17*). Common heterotrophs (e.g., *Saccharomyces cerevisiae*) are already used widely in industrial settings because of the large catalog of target metabolites accessible through genetic manipulation tools (*18*). The well-studied biology of canonical model organisms may provide access to better genetic and analytical tools to unravel the mechanisms governing electron transport and metabolic flux in biohybrid systems (*19*).

Of particular interest is the regeneration of the redox cofactor NADPH (reduced form of nicotinamide adenine dinucleotide phosphate), owing to its central role as a cosubstrate in biosynthetic pathways (*20*). This process is strongly intertwined with biomass production and is a common bottleneck in the production of metabolites through microbial cell factories (*21*). The primary source of NADPH in yeasts is the pentose phosphate pathway (PPP), which oxidizes a hexose sugar with concomitant loss of two equivalents of CO_2, decreasing theoretical carbon yields (*22*). Therefore, decoupling NADPH generation from central carbon metabolism may help maximize carbon flux for the production of desired metabolites (*20*).

We developed a *S. cerevisiae*–indium phosphide (InP) hybrid system, which combines rationally designed metabolic pathways and the electron donation capabilities of illuminated semiconductors (Fig. 1 and fig. S1). InP was selected as a photosensitizer in this biohybrid system because its direct bandgap (E_g = 1.34 eV) enables efficient absorption of a large fraction of the solar spectrum and is positioned appropriately to accept electrons from various species in the culture medium (fig. S2) (*23*). Additionally, its stability to oxygen and biocompatibility suggest that InP is an ideal material for biological integration (*24*). InP nanoparticles were prepared independently (fig. S3) and subsequently assembled on genetically engineered yeast cells by means of a biocompatible, polyphenol-based assembly method (*25*) (Fig. 1A and fig. S1). Yeast strain *S. cerevisiae* Δ*zwf1* was selected for the engineering of the biohybrid system. The deletion of the gene *ZWF1*, encoding the glucose-6-phosphate dehydrogenase enzyme, disrupts the oxidative portion of the PPP (*22*), causing a marked decrease in cytosolic NADPH generation capacity (Fig. 1B). We examined the integrated function of the biohybrid system to regenerate NADPH, which is essential for the biosynthesis of shikimic acid (SA), a precursor of aromatic amino acids (Fig. 1, C and D). *S. cerevisiae* Δ*zwf1* was genetically engineered to overexpress four genes to enhance carbon flux through the SA pathway (Fig. 1B) (*22*). The pentafunctional protein Aro1, which catalyzes the reduction of 3-dehydroshikimic acid (DHS) to SA, is selective for NADPH, and a low availability of cytosolic NADPH directly affects the production of SA, leading to elevated accumulation of its precursor, DHS. In previous examples of biohybrid systems, light-harvesting semiconductor particles attached to the surface of bacteria were able to provide reducing equivalents to central metabolic processes (*12*). We rationalized that the *S. cerevisiae* Δ*zwf1*–InP hybrid system (fig. S4) could operate similarly, with electrons flowing from the illuminated, surface-bound InP particles to the regeneration of NADPH from $NADP^+$ (nicotinamide adenine dinucleotide phosphate) inside the cell (Fig. 1, C and D). This regenerated NADPH can fuel the ultimate conversion of DHS to SA (*26*). Therefore, the *S. cerevisiae* Δ*zwf1*–InP hybrids both enable us to evaluate the efficiency of NADPH regeneration and lead to the enhanced biosynthesis of a highly sought-after molecule through photon energy conversion.

We designed a series of control experiments in which the presence of light and InP nanoparticles was varied (fig. S5). After 72 hours of aerobic growth, *S. cerevisiae* Δ*zwf1*–InP hybrids under illumination (5.6 mW cm^{-2}) (fig. S6) achieved the highest DHS-to-SA conversion rate with a SA/DHS ratio of 23.5 ± 1.6 (Fig. 2A and figs. S7 to S9). In contrast, a control experiment without illumination led to a ratio of only 0.67 ± 0.3 (fig. S10). Similarly, a low SA/DHS ratio was observed in the presence of InP nanoparticles that were not assembled on the cell surface, suggesting the importance of proximity in enabling photochemical synthesis. This is in line with recent reports describing the ability of cell wall–bound components in yeasts to contribute to extracellular electron transport through electron "hopping" mechanisms (*27*). In the absence of InP, *S. cerevisiae* Δ*zwf1* also showed a lower SA/DHS ratio, regardless of illumination scheme (figs. S11 and S12). The total SA production of the illuminated biohybrid system was superior to all other conditions, with a final titer of 48.5 ± 2.1 mg l^{-1}, showing an 11-fold increase compared with its counterpart with no illumination and a 24-fold increase compared with engineered cells in the presence of unattached InP nanoparticles (Fig. 2B). DHS-to-SA conversion yield also increased, to a point, with higher light intensities but decreased under the highest light intensity, possibly as a result of metabolic saturation or photodamage to the cells (fig. S13).

The SA/DHS ratio has previously been shown to serve as a metabolic readout for cytosolic levels

[1]Wyss Institute for Biologically Inspired Engineering, Harvard University, Boston, MA 02115, USA. [2]Department of Chemistry and Chemical Biology, Harvard University, Cambridge, MA 02138, USA. [3]Department of Systems Biology, Harvard Medical School, Boston, MA 02115, USA. [4]Department of Bioengineering, School of Engineering and Applied Sciences, University of Pennsylvania, PA 19104, USA. [5]John A. Paulson School of Engineering and Applied Sciences, Harvard University, Cambridge, MA 02138, USA. *Corresponding author. Email: junling.guo@wyss.harvard.edu (J.G.); neel.joshi@wyss.harvard.edu (N.S.J.) †These authors contributed equally to this work.

of NADPH/NADP$^+$ (*28*). The highest NADPH/NADP$^+$ ratio calculated for the illuminated biohybrid experiment reaches a value of 87.1 ± 6.0 (Fig. 2C). Notably, this value was higher than even that measured for InP-free and -integrated wild-type *S. cerevisiae*, which possesses the fully functional machinery to produce NADPH through the oxidative PPP (fig. S14). *S. cerevisiae* Δ*zwf1* in darkness showed the lowest NADPH/NADP$^+$ ratios, regardless of the presence of InP. These results support the contention that irradiated, cell surface–assembled InP can drive the regeneration of cofactor NADPH, facilitating the conversion of DHS to SA. As determined from colony-forming unit (CFU) assays on nutrient-rich solid media, cell viability did not differ before and after the assembly of InP nanoparticles (Fig. 2D), confirming the biocompatibility of the particle assembly protocol. During fermentation in selective minimal media, cell count decreased for the biohybrids, regardless of the illumination scheme (see supplementary materials for additional discussion).

To further evaluate the metabolic performance of the biohybrid systems, we characterized their ability to consume glucose and variations in carbon flux. Glucose was fully consumed by the bare cells during the first 24 hours, whereas nearly 25% of the total initial glucose remained unused in the complete biohybrid scheme (Fig. 3A). The SA production kinetics in the *S. cerevisiae* Δ*zwf1*–InP hybrids showed that the conversion of DHS to SA occurred throughout the entire illumination period (Fig. 3B), suggesting a continuous supply of NADPH and potential accumulation of biosynthetic intermediates along the SA pathway that lags behind glucose consumption (*29*). This finding was also supported by the consistently high mass fractions of SA (~90%). The specific SA yields of *S. cerevisiae* Δ*zwf1*–InP hybrids surpassed those of the *S. cerevisiae* Δ*zwf1* and the wild-type bare cells cultured in darkness (Fig. 3C). The light-to-SA conversion efficiency reached a maximum of 1.58 ± 0.05% 12 hours after the start of fermentation and dropped as SA production plateaued (fig. S15). To unravel the variations in the central carbon metabolism caused by the illumination of InP in the biohybrids, we measured the production of secreted by-products, including ethanol and glycerol, linked to other pathways (figs. S16 and S17). Figure 3D shows that the concentration of these by-products produced by the illuminated biohybrids (C_L) was lower than its counterpart under dark conditions (C_D). This implies that the surface-assembled, photoexcited InP shunts carbon in *S. cerevisiae* Δ*zwf1* toward the desired SA pathway, with less activity in alternative pathways for NADPH regeneration (e.g., pathways catalyzed by aldehyde dehydrogenase) (Fig. 3E).

Though membrane-bound hydrogenases have been invoked to explain the ability of previously reported analogous bacterial systems to make use of photogenerated electrons (*29*–*31*), *S. cerevisiae* is surrounded by a cell wall composed of extracellular polymeric substances that would prevent direct contact between membrane-bound proteins and the InP particles. The need for proximity between InP particles and the cells suggests that the cell wall might mediate electron transfer in our biohybrids (*27*). Differential pulse voltammetry performed on the spent medium after fermentation (Fig. 3F and fig. S18) exhibited peaks more negative of the thermodynamic potential for NADP$^+$/NADPH [E° = −0.324 V versus normal hydrogen electrode (NHE) at pH 7]. This higher redox activity after *S. cerevisiae* Δ*zwf1* growth suggests that soluble redox-active species likely also play a role in electron transfer, as has been reported for yeast-based microbial fuel cells without exogenous mediators (*32*). The electron transfer mechanism in these *S. cerevisiae* Δ*zwf1*–InP hybrids remains an active subject of investigation, as multiple possible mechanisms (e.g., soluble mediators and cell wall–bound redox mediators) could exist in our biohybrid system.

The development of inorganic-biological hybrid systems in yeast will enable expansion of this overall approach to the production of higher-value metabolites. For example, the production of benzylisoquinoline alkaloids, which is already established in yeast, requires the activity of more than 10 membrane-bound cytochrome P450 oxidoreductases that depend on NADPH as an electron donor (*18*). The technology presented in this work may thus elevate the production efficiency of alkaloid natural products and other drugs and nutraceuticals, though practical implementation

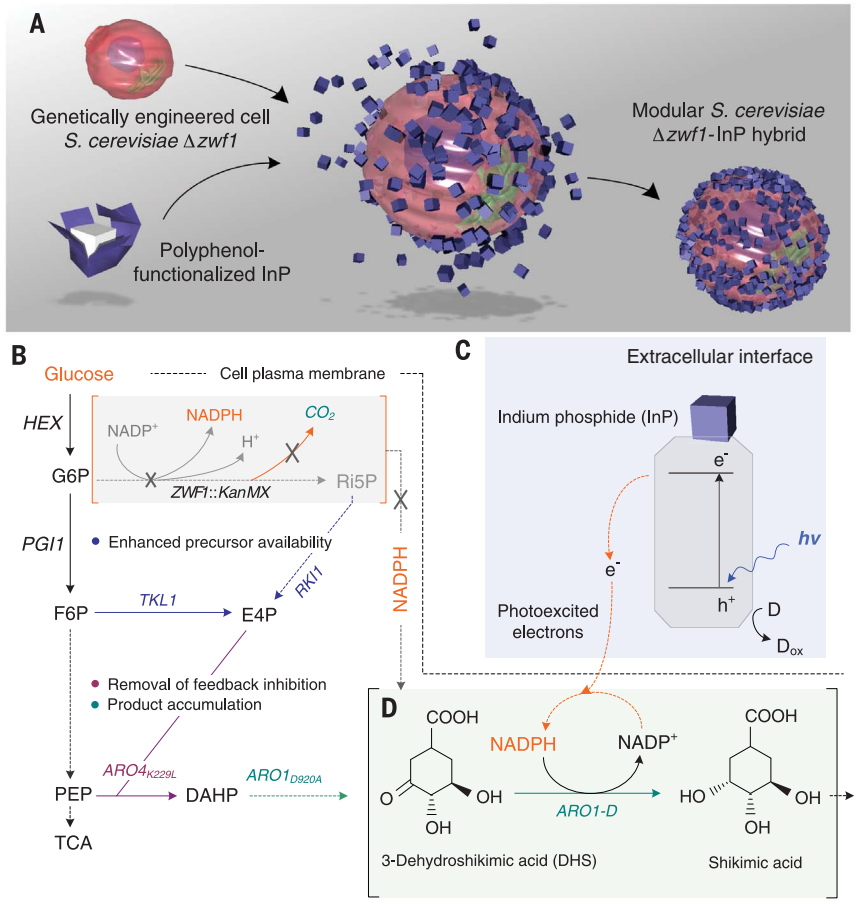

Fig. 1. Assembly of *S. cerevisiae*–InP hybrids and rationally designed metabolic pathways. (**A**) InP nanoparticles were first functionalized with polyphenol moieties and then assembled on the surface of genetically engineered yeast to form modular inorganic-biological hybrids. (**B**) Metabolic engineering scheme for overproduction of SA. *S. cerevisiae* Δ*zwf1* has the oxidative PPP disrupted (*ZWF1*), leading to low cytosolic NADPH pools, which directly affects the SA pathway and reduces carbon loss in the form of CO_2. (**C** and **D**) Schematic of cellular NADPH regeneration and SA biosynthesis assisted by photogenerated electrons from InP nanoparticles. G6P, glucose-6-phosphate; F6P, fructose-6-phosphate; Ri5P, ribulose-5-phosphate; E4P, erythrose-4-phosphate; PEP, phosphoenolpyruvate; DAHP, 3-deoxy-D-arabinoheptulosonate-7-phosphate; HEX, hexokinase; ZWF1, glucose-6-phosphate 1-dehydrogenase; PGI1, phosphoglucose isomerase; RKI1, ribose-5-phosphate ketol-isomerase; TKL1, transketolase; $ARO4_{K229L}$, feedback-insensitive DAHP synthase; $ARO1_{D920A}$, mutant pentafunctional aromatic enzyme; TCA, tricarboxylic acid cycle; h, Planck's constant; ν, frequency; h^+, electron hole; e^-, electron; D, putative electron donors in the cell culture medium; D_{ox}, oxidized electron donor species.

will require the development of illumination sources that interface with scaled-up fermenters. Our synthetic scheme is highly modular, enabling a mix-and-match approach; makes use of cheap components; and is compatible with existing workhorse cellular chassis and a wide range of particle-cell combinations. A more thorough understanding of electron transport mechanisms and global changes to metabolic flux will undoubtedly facilitate design and implementation of even better biohybrid systems. These systems would make use of alternative energy sources to streamline metabolic efficiency. With an ever-growing set of genetic tools, functional nanoparticles, and cell types, modular biohybrid platforms are likely to enable efficient and economical biochemical production of valuable and challenging targets.

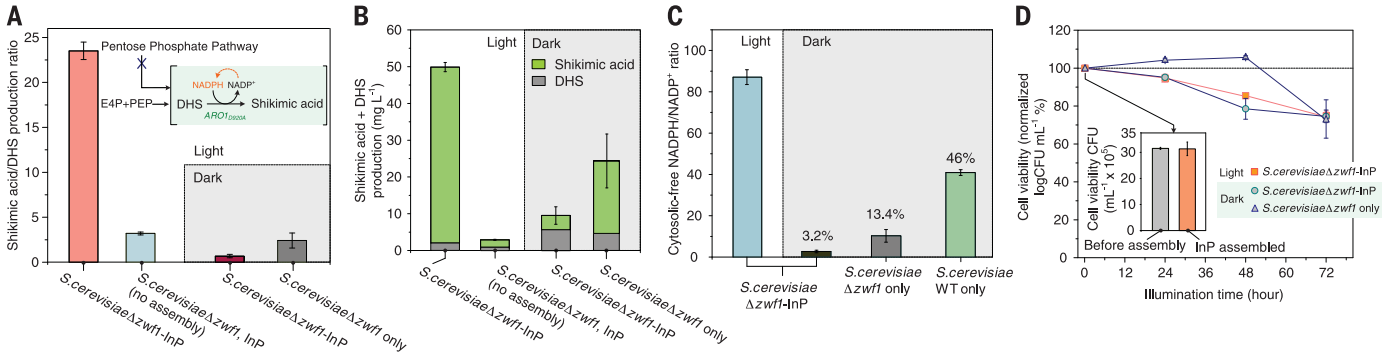

Fig. 2. Physiological and metabolic characterization of the *S. cerevisiae*–InP hybrid system. (**A**) Comparison of SA/DHS ratios in biohybrids and in yeast-only fermentations with light and dark conditions. (**B**) Total accumulation of SA and DHS after 72 hours of growth. (**C**) Estimation of cytosolic-free NADPH/NADP$^+$ ratio, based on the conversion of DHS to SA. (**D**) Cell viability assay based on counting of CFU, performed on rich solid media. The inset shows that the preparation of the biohybrids does not affect the initial CFU amount. Variation is represented by SE (error bars) from three independent replicates for all data points.

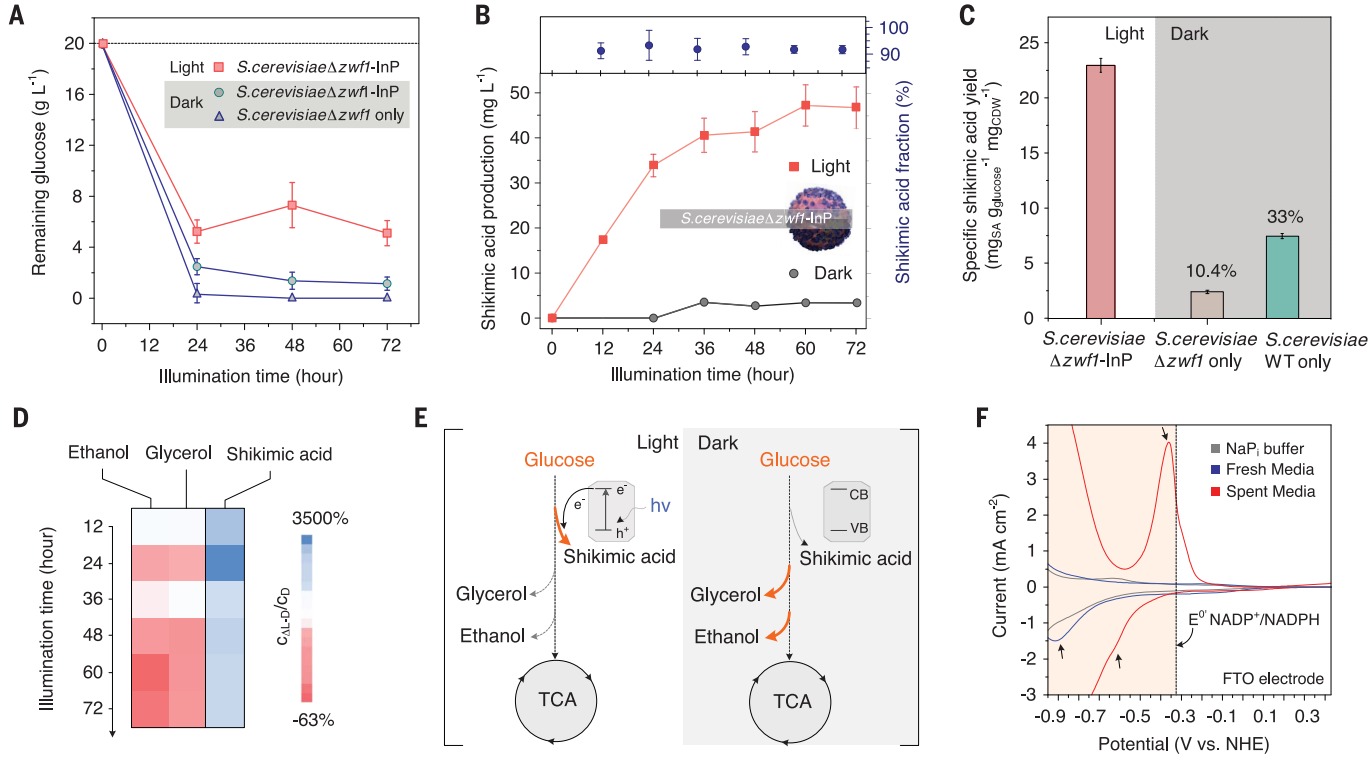

Fig. 3. Carbon utilization, cytosolic-free NADPH, and electron transfer in the *S. cerevisiae*–InP hybrid system. (**A**) Glucose consumption over the course of 72-hour culture. (**B**) SA production profiles in light and dark conditions. SA/DHS conversion yield was expressed as a mass fraction: [SA]/([SA] + [DHS]). (**C**) Specific SA yield based on consumed glucose and cell dry weight (CDW). (**D**) Percent variation in SA and by-product formation of the biohybrids under light (C_L) versus dark (C_D) conditions over time. (**E**) Proposed metabolic flux distributions based on total SA plus DHS concentrations and by-product (glycerol and ethanol) formation. CB, conduction band; VB, valence band. (**F**) Differential pulse voltammetry of culture medium before and after *S. cerevisiae* Δ*zwf1* growth. Arrows indicate electrochemical signatures from possible species with sufficient reducing potential to convert NADP$^+$ to NADPH. NaPi, sodium phosphate; FTO, fluorine-doped tin oxide. Variation is represented by SE (error bars) from three independent replicates for all data points.

REFERENCES AND NOTES

1. R. E. Blankenship *et al.*, *Science* **332**, 805–809 (2011).
2. K. K. Sakimoto, N. Kornienko, P. Yang, *Acc. Chem. Res.* **50**, 476–481 (2017).
3. A. Le Goff *et al.*, *Science* **326**, 1384–1387 (2009).
4. E. Reisner, D. J. Powell, C. Cavazza, J. C. Fontecilla-Camps, F. A. Armstrong, *J. Am. Chem. Soc.* **131**, 18457–18466 (2009).
5. K. A. Brown, M. B. Wilker, M. Boehm, G. Dukovic, P. W. King, *J. Am. Chem. Soc.* **134**, 5627–5636 (2012).
6. J. P. Giraldo *et al.*, *Nat. Mater.* **13**, 400–408 (2014).
7. S. F. Rowe *et al.*, *ACS Catal.* **7**, 7558–7566 (2017).
8. C. Liu, K. K. Sakimoto, B. C. Colón, P. A. Silver, D. G. Nocera, *Proc. Natl. Acad. Sci. U.S.A.* **114**, 6450–6455 (2017).
9. K. A. Brown *et al.*, *Science* **352**, 448–450 (2016).
10. C. Liu, B. C. Colón, M. Ziesack, P. A. Silver, D. G. Nocera, *Science* **352**, 1210–1213 (2016).
11. E. M. Nichols *et al.*, *Proc. Natl. Acad. Sci. U.S.A.* **112**, 11461–11466 (2015).
12. K. K. Sakimoto, A. B. Wong, P. Yang, *Science* **351**, 74–77 (2016).
13. H. Li *et al.*, *Science* **335**, 1596 (2012).
14. W. Wei *et al.*, *Sci. Adv.* **4**, eaap9253 (2018).
15. M. J. Herrgård *et al.*, *Nat. Biotechnol.* **26**, 1155–1160 (2008).
16. J. Förster, I. Famili, P. Fu, B. Ø. Palsson, J. Nielsen, *Genome Res.* **13**, 244–253 (2003).
17. J. D. Keasling, *Science* **330**, 1355–1358 (2010).
18. S. Galanie, K. Thodey, I. J. Trenchard, M. Filsinger Interrante, C. D. Smolke, *Science* **349**, 1095–1100 (2015).
19. J. Nielsen, J. D. Keasling, *Cell* **164**, 1185–1197 (2016).
20. X. Wang *et al.*, *Chem* **2**, 621–654 (2017).
21. S. Li, Y. Li, C. D. Smolke, *Nat. Chem.* **10**, 395–404 (2018).
22. M. Suástegui *et al.*, *Metab. Eng.* **42**, 134–144 (2017).
23. A.-M. Van Wezemael, W. Laflere, F. Cardon, W. Gomes, *J. Electroanal. Chem. Interfacial Electrochem.* **87**, 105–109 (1978).
24. K. K. Sakimoto *et al.*, *J. Am. Chem. Soc.* **140**, 1978–1985 (2018).
25. J. Guo *et al.*, *Nat. Nanotechnol.* **11**, 1105–1111 (2016).
26. M. Suástegui, W. Guo, X. Feng, Z. Shao, *Biotechnol. Bioeng.* **113**, 2676–2685 (2016).
27. Y. Xiao *et al.*, *Sci. Adv.* **3**, e1700623 (2017).
28. J. Zhang *et al.*, *Sci. Rep.* **5**, 12846 (2015).
29. N. Kornienko *et al.*, *Proc. Natl. Acad. Sci. U.S.A.* **113**, 11750–11755 (2016).
30. M. B. Wilker *et al.*, *J. Am. Chem. Soc.* **136**, 4316–4324 (2014).
31. K. Pandey, S. T. Islam, T. Happe, F. A. Armstrong, *Proc. Natl. Acad. Sci. U.S.A.* **114**, 3843–3848 (2017).
32. Y. Hubenova, M. Mitov, *Bioelectrochemistry* **106**, 177–185 (2015).

ACKNOWLEDGMENTS

We thank J. Richardson, G. Bazan, C. Catania, B. Tardy, and Y. Klyachina for helpful discussions; the group of Z. Shao at Iowa State University for providing the shikimic acid constructs; and E. Benecchi and M. Ericsson at the Harvard Medical School electron microscopy facility for help on microtoming techniques. Work was performed in part at the Center for Nanoscale Systems at Harvard University and the NSF's National Nanotechnology Infrastructure Network (NNIN). **Funding:** Work in the N.S.J. laboratory is supported by the National Institutes of Health (1R01DK110770-01A1) and the Wyss Institute for Biologically Inspired Engineering at Harvard University. D.G.N. acknowledges funding support from the National Institutes of Health (GM 47274). K.K.S. acknowledges the Harvard University Center for the Environment Fellowship for support. **Authors contributions:** J.G., M.S., and N.S.J. conceived of the idea. All authors performed research and/or analyzed data. J.G., M.S., N.S.J., K.K.S., and D.G.N. wrote and/or edited the manuscript. **Competing interests:** J.G., N.S.J., and M.S. are inventors on patent application 62691397 submitted by Harvard University and the Wyss Institute that covers photochemical biosynthesis enabled by biohybrids of the type described in this paper. **Data and materials availability:** All data are available in the main text or the supplementary materials. The primary strain used in this study, *S. cerevisiae* BY4741 zwf1Δ (MATa, his3Δ1, leu2Δ0, met15Δ0, ura3Δ0, zwf1Δ::KanMX), was obtained under an MTA from Iowa State University.

SUPPLEMENTARY MATERIALS

www.sciencemag.org/content/362/6416/813/suppl/DC1
Materials and Methods
Supplementary Text
Figs. S1 to S19
References (*33*–*35*)

14 June 2018; accepted 1 October 2018
10.1126/science.aat9777

Light-driven fine chemical production in yeast biohybrids

Junling Guo, Miguel Suástegui, Kelsey K. Sakimoto, Vanessa M. Moody, Gao Xiao, Daniel G. Nocera and Neel S. Joshi

Science **362** (6416), 813-816.
DOI: 10.1126/science.aat9777

Light-powered cell factories

Bacteria and fungi are used industrially to produce commodity fine chemicals at vast scale. Sugars are an economical feedstock, but many of the desired products require enzymatic reduction, meaning that some of the sugar must be diverted to regenerate the cellular reductant NADPH (reduced form of nicotinamide adenine dinucleotide phosphate). Guo *et al.* show that electrons from light-sensitive nanoparticles can drive reduction of cellular NADPH in yeast, which can then be used for reductive biosynthetic reactions. This system can reduce diversion of carbon to NADPH regeneration and should be compatible with many existing engineered strains of yeast.

Science, this issue p. 813